

Present and Future of Super High Efficiency Multi-Junction Solar Cells

Masafumi Yamaguchi^{*a}, Tatsuya Takamoto^b, Kenji Araki^c

^aToyota Technological Institute, 2-12-1 Hisakata, Tempaku, Nagoya 468-8511, Japan

^bSharp Corporation, Hajikami, Shinjo, Nara 639-2198, Japan

^cDaido Steel Corporation, Daido-cho, Minami, Nagoya 457-8545, Japan

*E-mail:masafumi@toyota-ti.ac.jp; phone 81-52-809-1875; fax 81-52-809-1879;

ABSTRACT

While single-junction solar cells may be capable of attaining AM1.5 efficiencies of up to 29%, multi-junction (MJ, Tandem) III-V compound solar cells appear capable of realistic efficiencies of up to 50% and are promising for space and terrestrial applications. In fact, the InGaP/GaAs/Ge triple-junction solar cells have been widely used for space since 1997. In addition, industrialization of concentrator solar cell modules using III-V compound MJ solar cells have been announced by some companies. This paper presents principles and key issues for realizing high-efficiency MJ solar cells, issues relating to development and manufacturing, and applications for space and terrestrial uses.

Keywords: III-V compounds, multi-junction solar cells, high conversion efficiency, terrestrial and space applications

1. INTRODUCTION

Multi-junction (MJ, Tandem) solar cells are composed of multi-layers with different bandgap energies are shown in figure 1 and have the potential for achieving high conversion efficiencies of over 50% and are promising for space and terrestrial applications due to wide photo response. Figure 2 shows theoretical conversion efficiencies of single-junction and multi-junction (MJ) solar cells in comparison with experimentally realized efficiencies.

Tandem solar cells were proposed in 1955 by Jackson [1] and in 1960 by Wolf [2]. Table 1 shows progress of the III-V compound multi-junction solar cell technologies. MIT group [3] encouraged R&D of tandem cells based on their computer analysis.

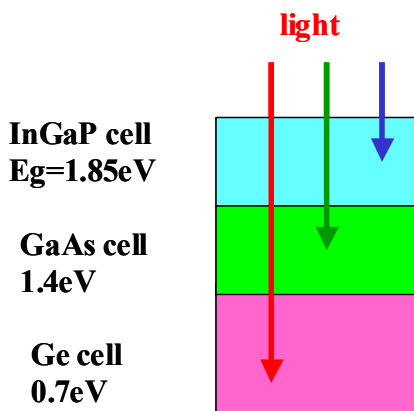


Fig. 1. A schematic structure of a multi-layer solar cell.

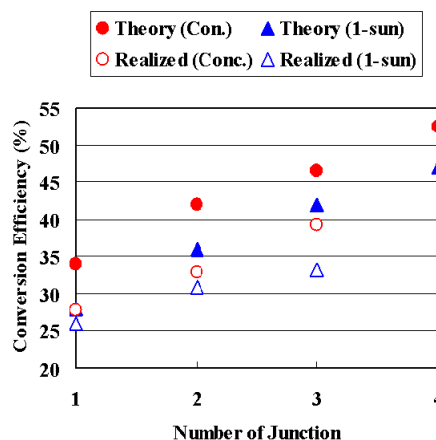


Fig. 2. Theoretical and experimentally realized conversion efficiencies of single-junction and multi-junction solar cells.

Table 1. Progress of the III-V compound multi-junction solar cell technologies.

1955 1960	Proposal of multi-junction solar cell	Jackson Wolf
1982	Efficiency calculation of tandem cells	MIT
1982	15.1% AlGaAs/GaAs 2-junction (2-J) cell	RTI
1987	Proposal of double-hetero structure tunnel junction for multi-junction interconnection	NTT
1987	20.2% AlGaAs/GaAs 2-J cell	NTT
1989	32.6% GaAs//GaSb concentrator 2-J cell (mechanical-stacked, 100-suns concentration)	Boeing
1990	Proposal of InGaP as top a cell material	NREL
1990	27.3% InGaP/GaAs 2-J cell	NREL
1996	30.3% InGaP/GaAs 2-J cell	Jpn. Energy
1997	Discovery of radiation-resistance of InGaP top cell	Toyota Tech. Inst.
1997	33.3% InGaP/GaAs//InGaAs 3-J cell (mechanical-stacked)	Jpn. Energy, Sumitomo & Toyota Tech. Inst.
1997	Commercial satellite with 2-J cells	Hughes
2000	31.7% InGaP/InGaAs/Ge 3-J cell	Jpn. Energy
2003	39.2% InGaP/InGaAs/Ge 3-J cell (200-suns concentration)	Sharp
2004	28% large-area (7,000cm ²) InGaP/InGaAs/Ge 3-J cell module (outdoor)	Daido Steel, Daido Metal, Sharp & Toyota T.I.
2006	40.7% InGaP/GaAs/Ge 3-J cell (236-suns concentration)	Spectrolab

Although AlGaAs/GaAs tandem cells, including tunnel junctions and metal interconnectors, were developed in the early years, a high efficiency close to 20% was not obtained [4]. This is because of difficulties in making high performance and stable tunnel junctions, and the defects related to the oxygen in the AlGaAs materials [5]. A double hetero (DH) structure tunnel junction was found to be useful for preventing diffusion from the tunnel junction and improving the tunnel junction performance by the authors [6]. The authors demonstrated 20.2% efficiency AlGaAs/GaAs 2-junction cells [7]. An InGaP material for the top cell was proposed by NREL group [8]. As a result of performance improvements in tunnel junction and top cell, over 30% efficiency has been obtained with InGaP/GaAs 2-junction cells by authors [9]. Recently, InGaP/GaAs-based MJ solar cells have drawn increased attention for space applications because superior radiation-resistance of InGaP top cells and materials have been discovered by the authors [10] and those have the possibility of high conversion efficiency of over 30%. In fact, the commercial satellite (HS 601HP) with 2-junction GaInP/GaAs-on Ge solar arrays was launched in 1997 [11].

More recently, InGaP/GaAs-based MJ solar cells have drawn increased attention for terrestrial applications because concentrator operation of MJ cells have great potential of providing high performance and low-cost solar cell modules. For concentrator applications, grid structure has been designed in order to reduce the energy loss due to series resistance, and 39.2% (AM1.5G, 200-suns) efficiency has been demonstrated by Sharp [12]. Most recently, 40.7% efficiency has been reported with InGaP/GaAs/Ge 3-junction concentrator cells by Spectrolab [13]. In addition, the authors have realized high-efficiency and large-area (7,000cm²) concentrator InGaP/InGaAs/Ge 3-junction solar cell modules of an outdoor efficiency of 28% [14] as a result of developing high-efficiency InGaP/InGaAs/Ge 3-junction cells, low optical loss Fresnel lens and homogenizers, and designing low thermal conductivity modules. Some companies including Sharp [15] have announced to commercialize InGaP/GaAs/Ge 3-junction concentrator cell modules for terrestrial use. This paper presents principles and key issues for realizing high-efficiency MJ solar cells, issues relating to development and manufacturing, and applications for space and terrestrial uses.

2. Key issues for realizing high-efficiency MJ solar cells

Key issues for realizing high-efficiency MJ tandem cells are discussed based on our results.

2.1 Selection of cell materials and improving the quality

MJ cells with different band gaps are stacked in tandem so that the cells cover wide wavelength region from 300 nm to 1800 nm. Cell materials are selected by considering band gap energies close to the optimal band gap energy combination based on theoretical efficiency calculation, and by considering lattice matching to substrates and less impurity problems.

Figure 3 shows minority-carrier diffusion length dependence of GaAs single-junction solar cell efficiency. It is clear that the higher minority-carrier diffusion length L (minority-carrier lifetime $\tau = L^2 / D$, where D is minority-carrier diffusion coefficient) is substantially necessary to realize the higher efficiency solar cells.

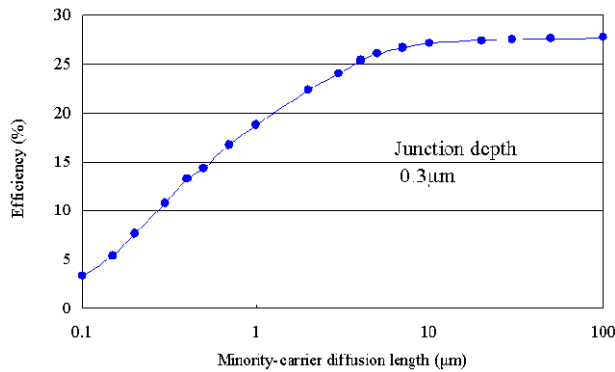


Fig. 3. Minority-carrier diffusion length dependence of GaAs single-junction solar cell efficiency.

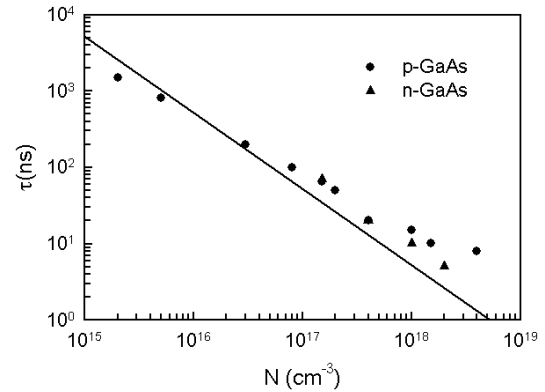


Fig. 4. Carrier concentration dependence of minority-carrier lifetime in p-type and n-type GaAs [16].

Figure 4 shows carrier concentration dependence of minority-carrier lifetime in p-type and n-type GaAs [16]. Minority-carrier lifetime τ is dependent on carrier concentration N of solar cell layers as expressed by

$$\tau = 1 / BN \quad (1)$$

where, B is radiative recombination coefficient. Therefore, carrier concentration of cell layers must be optimized by considering minority-carrier lifetime, build-in potential and series resistance of p-n junction diodes.

Selection of cell materials, especially selection of top cell materials is also important for high-efficiency tandem cells. It has been found by the authors [5] that oxygen-related defect in the AlGaAs top cell materials acts as the recombination center. As a top cell material latticed matched to GaAs or Ge substrates, InGaP has some advantages [8] such as lower interface recombination velocity, less oxygen problem and good window layer material compared to AlGaAs. The top cell characteristics depend on the minority carrier lifetime in the top cell layers. Figure 5 shows changes in photoluminescence (PL) intensity of the solar cell active layer as a function of the minority carrier lifetime τ of the p-InGaP base layer grown by MOCVD (metal-organic chemical vapor deposition) and surface recombination velocity (S).

The lowest S was obtained by introducing the AlInP window layer and the highest τ was obtained by introducing buffer layer and optimizing the growth temperature. The best conversion efficiency of the InGaP single-junction cell was 18.5 % [17].

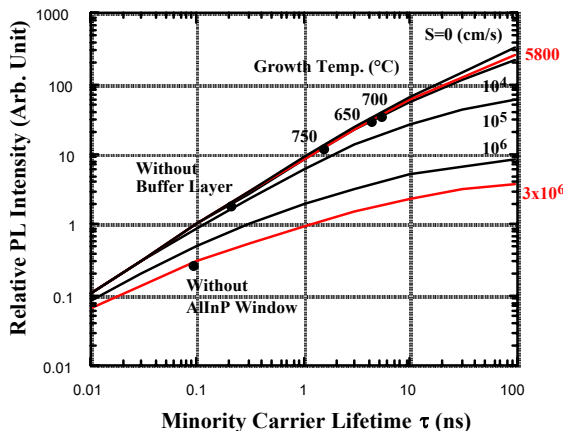


Fig. 5. Changes in photoluminescence (PL) intensity of the solar cell active layer as a function of the minority carrier lifetime τ of the p-InGaP base layer grown by MOCVD and surface recombination velocity (S).

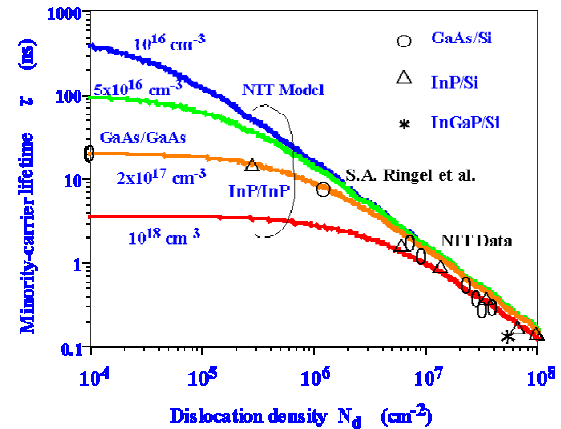


Fig. 6. Calculated and experimental dislocation density dependence of minority-carrier lifetime in GaAs, InP and InGaP.

2.2 Lattice matching between cell materials and substrates

Lattice mismatching of cell materials to substrates should be decreased because miss-fit dislocations must be generated in the upper cell layers and deteriorate cell efficiency. Figure 6 shows calculated and experimental dislocation density dependence of minority-carrier lifetime in GaAs [18]. Dislocation density N_d dependence of minority-carrier lifetime τ is expressed by the following equation [18]:

$$1/\tau = 1/\tau_r + 1/\tau_0 + \pi^3 DN_d / 4 \quad (2)$$

where τ_r is radiative recombination lifetime and τ_0 is minority-carrier lifetime associated with recombination at other unknown defects.

Application of InGaAs middle cell [19] lattice-matching to Ge substrates has demonstrated to increase open-circuit voltage (V_{oc}) due to lattice-matching and short-circuit current density (J_{sc}) due to decrease in bandgap energy of middle cell.

2.3 Effectiveness of wide bandgap back surface field (BSF) layer

Figure 7 shows surface recombination effect on short-circuit current density J_{sc} of $In_{0.14}Ga_{0.86}As$ homo-junction solar cells as a function of junction depth. Therefore, in order to improve efficiency drop attributed from front and rear surface recombination as shown in figure 8, formation of heteroface or double-hetero structure is necessary.

Figure 8 shows changes in V_{oc} and J_{sc} of InGaP single-junction cells as a function of potential barrier ΔE . Wide bandgap back-surface field (BSF) layer [19] is found to more effective for confinement of minority carriers compared to highly doped BSF layers.

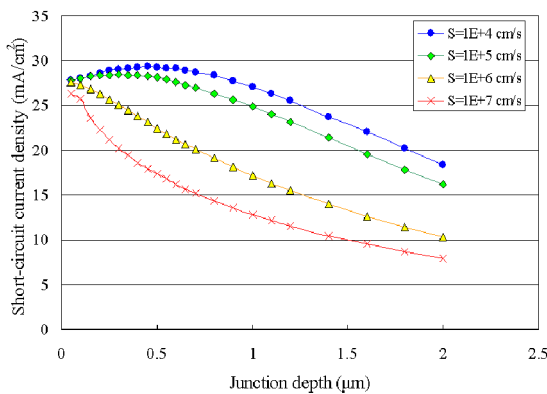


Fig. 7. Surface recombination effect on short-circuit current density J_{sc} of $In_{0.14}Ga_{0.86}As$ homo-junction solar cells as a function of junction depth.

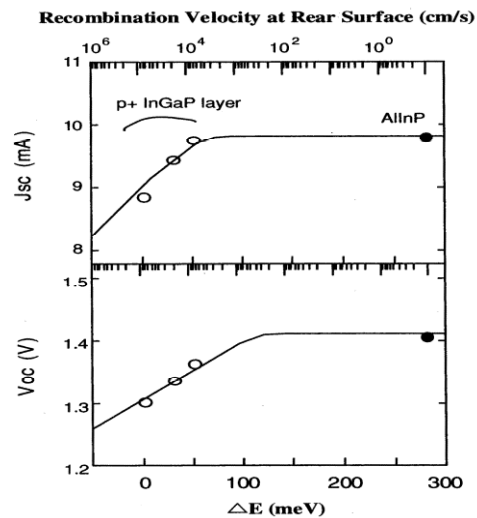


Fig. 8. Changes in V_{oc} and J_{sc} of InGaP single-junction cells as a function of potential barrier ΔE .

2.4. Low loss tunnel junction for intercell connection and preventing impurity diffusion from tunnel junction

Another important issue for realizing high-efficiency monolithic-cascade type tandem cells is the achievement of optically and electrically low-loss interconnection of two or more cells. A degenerately doped tunnel junction is attractive because it only involves one extra step in the growth process. To minimize optical absorption, formation of thin and wide-bandgap tunnel junctions is necessary as shown in figure 9. However, the formation of a wide-bandgap tunnel junction is very difficult because the tunneling current decreases exponentially with increase in bandgap energy.

In addition, impurity diffusion from a highly doped tunnel junction during overgrowth of the top cell increases the resistivity of the tunnel junction. As shown in figure 10, a double hetero (DH) structure was found to be useful for preventing diffusion by the authors⁶. An InGaP tunnel junction has been for the first time tried for an InGaP/GaAs tandem cell in our work [9]. As p-type and n-type dopants, Zn and Si were used, respectively. Peak tunneling current of the InGaP tunnel junction is found to increase from 5mA/cm^2 up to 2A/cm^2 by making a DH structure with AllnP barriers. Therefore, the InGaP tunnel junction has been observed to be very effective for obtaining high tunneling current, and DH structure has also been confirmed to be useful for preventing diffusion.

DH structure effect on suppression of impurity diffusion from the tunnel junction has been examined. Effective suppression of the Zn diffusion from tunnel junction by the InGaP tunnel junction with the AlInP-DH structure is thought to be attributed to the lower diffusion coefficient [20] for Zn in the wider bandgap energy materials such as the AlInP barrier layer and InGaP tunnel junction layer.

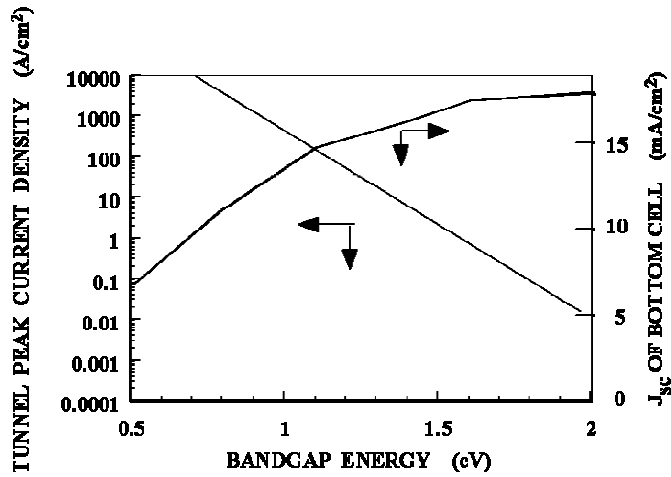


Fig. 9. Calculated tunnel peak current density and short-circuit current density J_{sc} of GaAs bottom cell as a function of bandgap energy of tunnel junction.

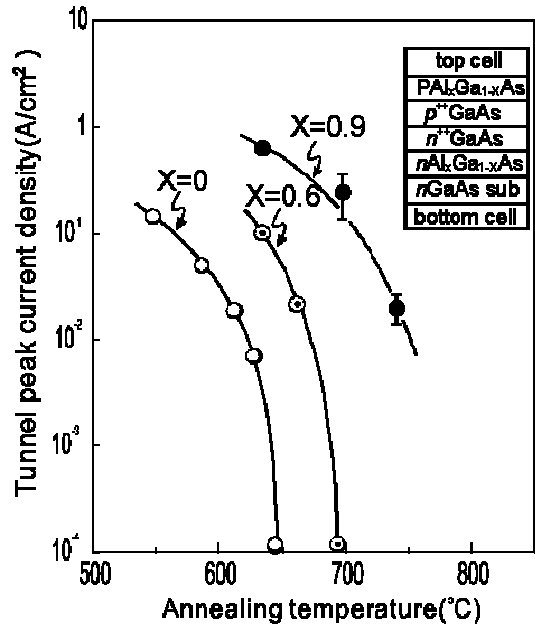


Fig. 10. Annealing temperature dependence of tunnel peak current densities for double hetero structure tunnel diodes. X is the Al mole fraction in $Al_xGa_{1-x}As$ barrier layers.

Table 2 summarizes key issues of realizing super-high-efficiency MJ solar cells.

Table 2. Key issues for realizing super high-efficiency multi-junction solar cells.

Key Issue	Past	Present	Future
Top cell materials	AlGaAs	InGaP	AlInGaP
3rd layer materials	None	Ge	InGaAsN etc.
Substrate	GaAs	Ge	Si
Tunnel junction	DH-structure GaAs tunnel J.	DH-structure InGaP tunnel J.	DH-structure InGaP or GaAs
Lattice matching	GaAs middle cell	InGaAs middle cell	(In)GaAs middle cell
Carrier confinement	InGaP-BSF	AlInP-BSF	Widgap-BSF
Photon confinement	None	None	Bragg reflector etc.

3. High-efficiency InGaP/GaAs/Ge 3-junction solar cells and their space applications

3.1 Development of high-efficiency InGaP/GaAs/Ge 3-junction solar cells

As one of the Sunshine Program in Japan, an R&D project for super high-efficiency MJ solar cells was started in 1990. Conversion efficiency of InGaP/GaAs based multijunction solar cells has been improved by the following technologies. A schematic illustration of the InGaP/(In)GaAs/Ge triple junction solar cell and key technologies for improving conversion efficiency are shown in figure 11.

3.1.1 Wide band-gap tunnel junction

A wide band-gap tunnel junction which consists of double-hetero structure p-Al(Ga)InP/p-AlGaAs/ n-(Al)InGaP/n-Al(Ga)InP increases incident light into the (In)GaAs middle cell and produces effective potential barriers for both minority-carriers generated in the top and middle cells. Both Voc and Isc of the cells are improved by the wide band-gap tunnel junction without absorption and recombination losses [9]. It is difficult to obtain high tunneling peak current with wide gap tunnel junction, so thinning depletion layer width by formation of highly doped junction is quite necessary. Since impurity diffusion is occurred during growth of the top cell [6], carbon and silicon which have low diffusion coefficient are used for p-type AlGaAs and n-type (Al)InGaP, respectively. Furthermore, the double-hetero structure supposes to suppress impurity diffusion from the highly doped tunnel junction [20]. The second tunnel junction between middle and bottom cells consists of p-InGaP/p-(In)GaAs/ n-(In)GaAs/n-InGaP which have wider band-gap than middle cell materials.

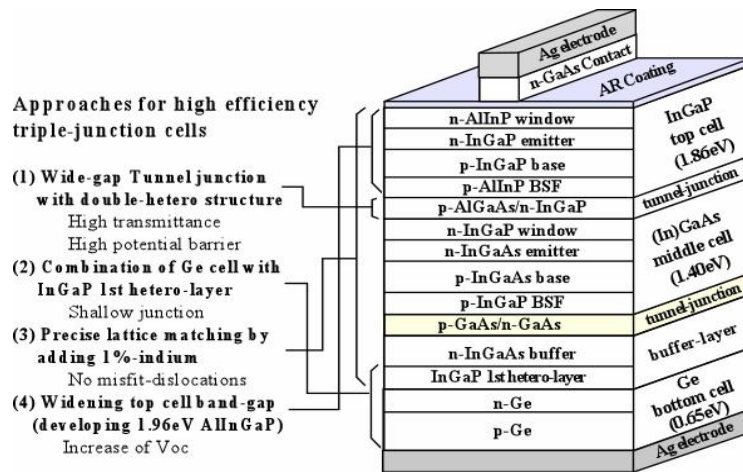


Fig. 11. Schematic illustration of a triple-junction cell and approaches for improving efficiency of the cell.

3.1.2 Heteroface structure Ge bottom cell

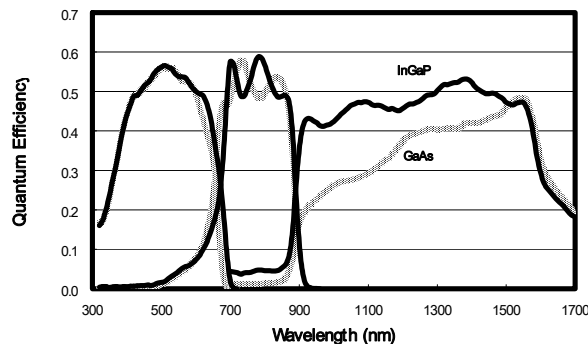


Fig. 12. Change in the spectral response due to modification of the 1st hetero-layer from GaAs to InGaP (without anti-reflection coating).

InGaP/GaAs cell layers are grown on a p-type Ge substrate. PN junction is formed automatically during MOCVD growth by diffusion of V-group atom from the first layer grown on the Ge substrate. So, the material of the first hetero layer is important for the performance of Ge bottom cell. An InGaP layer is thought to be suitable material for the first hetero layer, because phosphor has lower diffusion coefficient in Ge than arsenic and indium has lower solubility in Ge

than gallium. Figure 12 shows the change in spectral response of the triple-junction cell by changing the first hetero-growth layer on Ge from GaAs to InGaP. Quantum efficiency of the Ge bottom cell was improved by the InGaP hetero-growth layer. In the case of GaAs hetero-growth layer, junction depth was measured to be around 1 μ m. On the other hand, thickness of n-type layer produced by phosphor from the InGaP layer was 0.1 μ m. An increase in Ge quantum efficiency was confirmed to be due to a reduction in junction depth.

3.1.3 Precise lattice-matching to Ge substrate

Although 0.08% lattice-mismatch between GaAs and Ge was thought to be negligibly small, misfit-dislocations were generated in thick GaAs layers and deteriorated cell performance. By adding about 1% indium into the InGaP/GaAs cell layers, all cell layers are lattice-matched precisely to the Ge substrate. As a result, crosshatch pattern caused by misfit-dislocations due to lattice-mismatch was disappeared in the surface morphology of the cell with 1% indium, as shown in figure 13. The misfit-dislocations were found to influence not to I_{sc} but to V_{oc} of the cell. V_{oc} was improved by eliminating misfit-dislocations for the cell with 1% indium. In addition, wavelength of the absorption edge became longer and I_{sc} of both top and middle cells increased, by adding 1% indium.

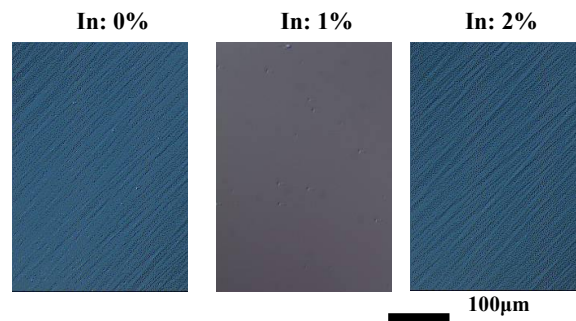


Fig. 13. Surface morphology of InGaAs with various indium compositions grown on Ge.

The best data of the triple-junction cells in our project are summarized in Table 3. Technologies described above 3.1.1-3.1.3 applied to fabrication of the triple junction cells. Band gap of the InGaP top cell of about 1.82 eV is still low. By using AlInGaP top cell with 1.96 eV, higher V_{oc} close to 2.72 V is predicted. Conversion efficiencies over 33% (AM1.5G) and close to 31% (AM0) will be expected for the (Al)InGaP/InGaAs/Ge triple junction cells.

Table 3. Characteristics of the triple-junction cells.

V_{oc} (mV)	J_{sc} (mA/cm ²)	FF	Efficiency (%)	Condition
2567	14.1	0.87	31.5	AM1.5G, 25 ⁰ C
2568	17.9	0.86	29.2	AM0, 28 ⁰ C

3.2 Radiation-resistance of InGaP-based MJ solar cells

Figure 14 shows effectiveness of radiation-resistance and high conversion efficiency of space cells from the point view of power density. Since radiation in space is severe, particularly in the Van Allen radiation belt, lattice defects are induced in semiconductors due to high-energy electron and proton irradiations, and the defects cause a decrease in the output power of solar cells. Further improvements in conversion efficiency and radiation-resistance of space cells are necessary for widespread applications of space missions. Recently, InGaP/GaAs-based MJ solar cells have drawn increased attention because of the possibility of high conversion efficiency of over 40% and radiation-resistance. An AM0 efficiency of 29.2% has been demonstrated for an InGaP/InGaAs/Ge 3-junction cell (4cm²) [12] as shown in Table 3.

Figure 15 shows the maximum power recovery due to light illumination of 100 mW/cm² at various temperatures for 1-MeV electron-irradiated InGaP/GaAs tandem cells [10]. The ratios of maximum power after injection, P_1 , to maximum

power before irradiation, P_0 , are shown as a function of injection time. Even at room temperature, photo injection-enhanced annealing of radiation damage to InGaP/GaAs tandem cells was observed. The recovery ratio increases with an increase in ambient temperature within the operating range for space use. Such a recovery is found to be attributed from damage recovery in InGaP top cell layer [10]. Therefore, the results show that InGaP/GaAs tandem cells under device operation conditions have superior radiation-resistant properties.

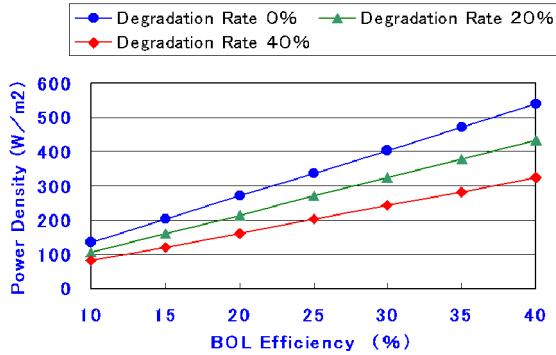


Fig. 14. Effectiveness of radiation-resistance and high conversion efficiency of space cells from the point view of power density.

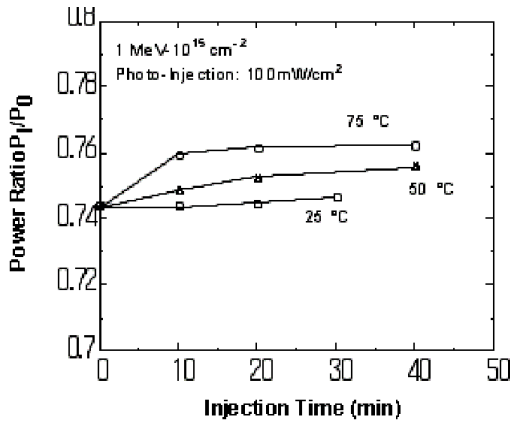


Fig. 15. The maximum power recovery of the InGaP/GaAs tandem cell due to light illumination at various temperatures.

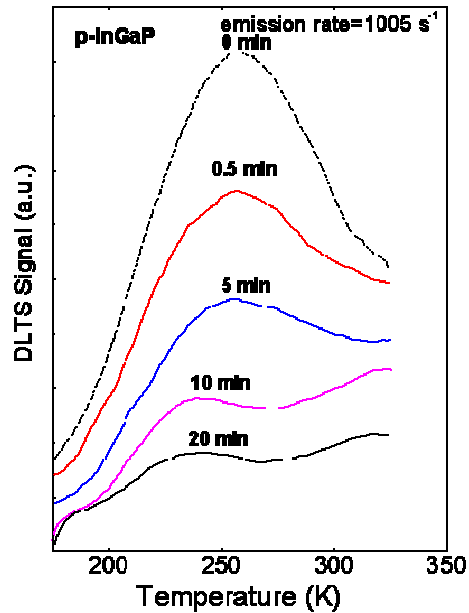


Fig. 16. DLTS spectrum of Trap (H2 $E_v+0.55eV$) for various injection times at 25°C with an injection density of 100mA/cm².

Figure 16 shows DLTS (Deep Level Transient Spectroscopy) spectrum of Trap H2 ($E_v+0.55eV$) for various injection times at 25°C with an AM1.5 light intensity of 100mA/cm². It is also found [21] by DLTS measurements that a major defect level H2 ($E_v+0.55eV$) recovers by forward bias or light illumination. Moreover, the H2 center is confirmed to act as a recombination center by using the double carrier pulse DLTS method. The enhancement of defect annealing in InGaP top cell layer under minority-carrier injection conditions is thought to occur as a result of the nonradiative electron-hole recombination process [22] whose energy E_R enhances the defect motion. The thermal activation energy E_A (1.1eV) of the defect is reduced to E_I (0.48~0.54eV) by an amount E_R (0.56~0.62eV). Thus electronic energy from a recombination event can be channeled into the lattice vibration mode which drives the defect motion: $E_I = E_A - E_R$.

3.3 Space applications of InGaP/GaAs/Ge 3-junction solar cells

Advanced technologies for high efficiency cells and discovery of superior radiation-resistance of InGaP based materials are thought to contribute to industrialization of InGaP-based multijunction space solar cells in Japan. Figure 17 shows Sharp space solar cell conversion efficiency heritage. Since 2002, InGaP/GaAs/Ge 3-junction solar cells have been commercialized for space use in Japan.

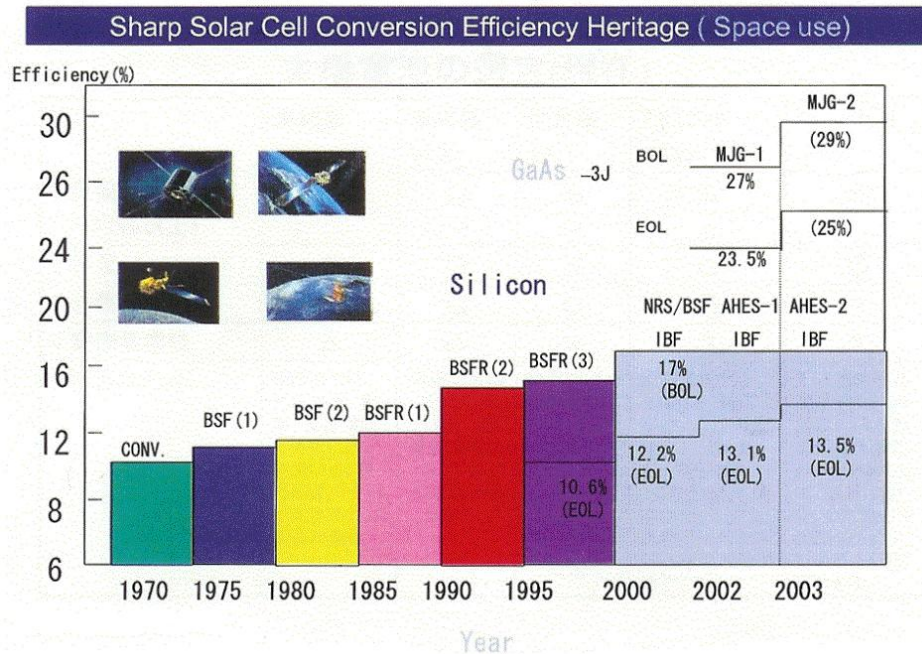


Fig. 17. Sharp space solar cell conversion efficiency heritage.

4. High efficiency concentrator InGaP/GaAs/Ge 3-junction solar cells and terrestrial applications

In order to apply a high efficiency multijunction cell developed for 1 sun condition to a concentrator cell operating under ~500suns condition, reduction in energy loss due to series resistance is the most important issue. Cell size was determined to be 7mm x 7mm with considering total current flow. Grid electrode pitching, height and width were designed in order to reduce series resistance. Figure 18 shows fill factor (FF) of the cell with various grid pitching under 250 suns. Grid electrode with 5 μ m height and 5 μ m width was made of Ag. Grid pitching influences lateral resistance between two grids (RL) and total electrodes resistance (RE). Series resistance of the cell (RS), RE and RL are also shown in figure 18. RE was measured directly after removing electrode from the cell by chemical etching. RL was calculated by using sheet resistance of window and emitter layers. Based on the data in figure 18, the grid pitching is determined to be 0.12 mm at this time. In order to reduce series resistance down to 0.01 Ω and obtain high FF under 500 suns, grid height should be increased to be twice. High efficiency under <500 suns is thought to be obtained by the optimal grid design without modification of the cell layer.

For concentrator applications, the grid structure has been designed in order to reduce the energy loss due to series resistance as shown in figure 18. Most recently, we have successfully fabricated high efficiency concentrator InGaP/InGaAs/Ge 3-junction solar cells designed for 500-sun application. The efficiencies by in-house measurement are 39.2 % at 200-suns and 38.9% at 489-suns as shown in figure 19 [12]. The solar simulator was equipped with both Xe lamp and halogen lamp and adjusted AM1.5G spectrum.

Concentrator InGaP/GaAs/Ge 3-junction solar cell modules have also been developed for terrestrial use [14]. A new concentrator optics is introduced, consist of a non-imaging dome-shaped Fresnel lens, and a kaleidoscope homogenizer. The non-imaging Fresnel lens allows wide acceptance half angle with keeping the same optical efficiency with minimum chromatic aberration. The homogenizer reshapes the concentrated into square solar cell aperture, mixed rays to uniform flux. Injection molding, is capable of manufacturing thousands of lenses in a single day and by a single machine. The

drawback of this method is difficulty of creating precise prism angles and flat facets. The maximum efficiency was a little above 80 % and overall efficiency was 73 %. After improvement of the process conditions, the averaged efficiency raised to 85.4 %.

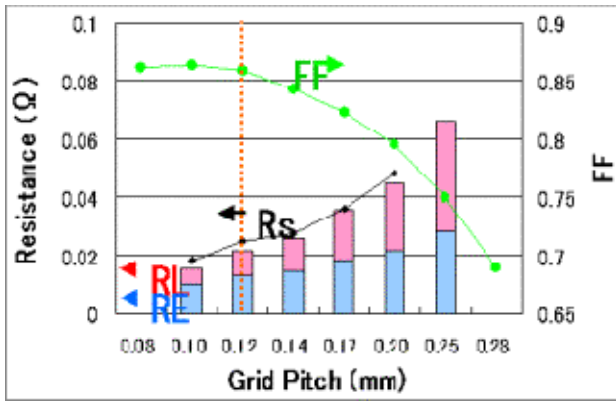


Fig. 18. FF of the concentrator cells with various grids pitching under 250-suns light. Series resistance (Rs), lateral resistance (RL) and total electrodes resistance (RE) are also shown.

A new packaging structure for III-V concentrator solar cells is developed, applicable mainly to Fresnel lens concentrator modules but may also be used in dish concentrator systems. The solar cell used in the new receiver package is III-V 3-junction concentrator solar cell developed. It is grown on a fragile Ge substrate with thickness of only 150 μm. The overall size was 7 mm X 9 mm with 7 mm square aperture area.

In addition, the following technologies have been developed:

- 1) Super-high pressure and vacuum-free lamination of the solar cell that suppresses the temperature rise to 20 degrees under 550 X geometrical concentration illumination of sunbeam.
- 2) Direct and voids-free soldering technologies of the fat metal ribbon to the solar cell, suppressing hot-spots and reducing the resistance, thereby allowing a current 400 times higher than normal nonconcentration operation to be passed with negligible voltage loss.
- 3) A new encapsulating polymer that survives exposure to high concentration UV and heat cycles.

The concentrator module is designed with ease of assembly in mind. All the technologically complex components are packaged into a receiver so that a series of receivers and lenses can be assembled with standard tools, using local materials and workforce. The concept is similar to the computer and automobile assembly industries, where key components are imported but the product assembled locally. It is anticipated that this approach will reduce the manufacturing cost of the module as shown in figure 20.

The peak uncorrected efficiency for the 7,056 cm² 400 X module with 36 solar cells connected in series was 26.6 %, measured in house. The peak uncorrected efficiencies for the same type of module with 6 solar cells connected in series and 1,176 cm² area measured by Fraunhofer ISE and NREL were 27.4 % and 24.9 %. The 5,445 cm² 550 X modules

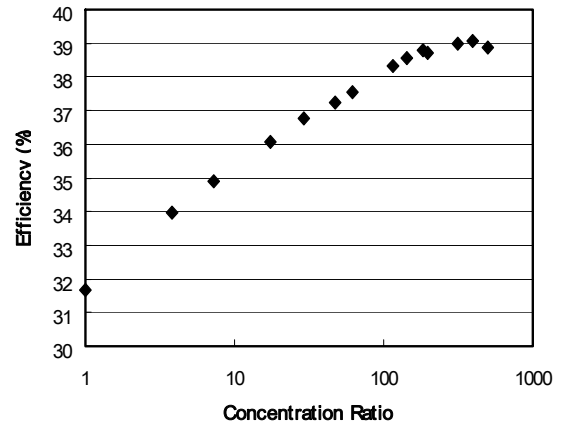


Fig. 19. Efficiency of a high-efficiency InGaP/InGaAs/Ge 3-junction cell vs. number of suns.

- 4) Beam-shaping technologies that illuminate the square aperture of the solar cell, from a round concentration spot.
- 5) Homogeniser technologies that give a uniform flux and prevent the conversion losses that stem from chromatic aberration and flux intensity distribution.

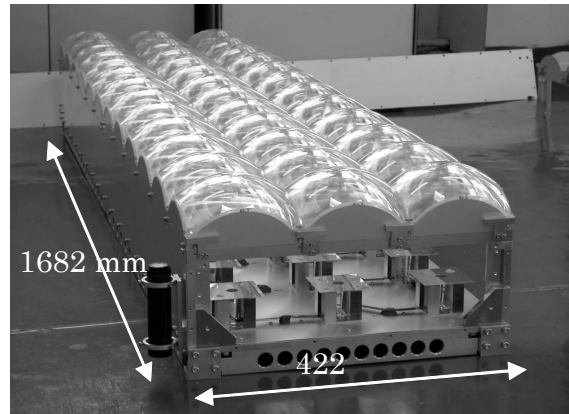


Fig. 20. Inside of the 400 X concentrator module with 36 receivers connected in series.

have also demonstrated 27-28.9%, measured in house. Table 4 summarizes the measured efficiency in three different sites.

A new 400X and 550X (geometrical concentration ratio) are developed and show the highest efficiency in any types of PV as well as more than 20 years of accelerated lifetime. This achievement is blessed with new innovative concentrator technologies. The new concentrator system is expected to open a door to a new age of high efficiency PV.

Table 4. Uncorrected peak efficiency measurement.

Concentration	Area cm ²	Site	Ambient	Uncorrected Efficiency	DNI W/m ²
400 X	7,056	Inuyama, Japan Manufacturer	29 C	27.6 %	810
400 X	7,056	Toyohashi, Japan Independent	7 C	25.9 %	645
400 X	1,176	Fraunhofer ISE, Germany Independent	19 C	27.4 %	839
400 X	1,176	NREL, USA Independent	29 C	24.9 %	940
550 X	5,445	Inuyama, Japan Manufacturer	33 C	28.9 %	741
550 X	5,445	Toyohashi, Japan Independent	28 C	27 %	777

5. Future Direction

Multi-junction solar cells will be widely used in space because of their high conversion efficiency and better radiation-resistance. In order to apply super high-efficiency cells widely, it is necessary to improve their conversion efficiency and reduce their cost.

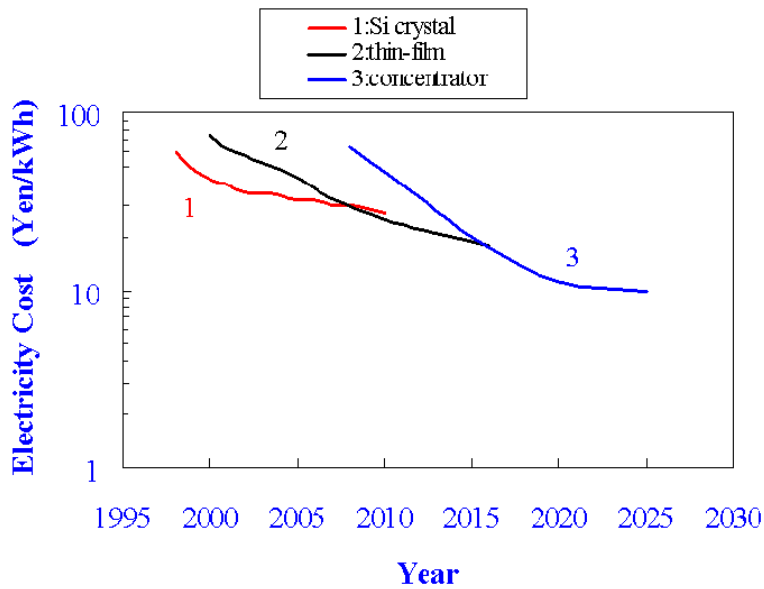


Fig. 21. Scenario of electricity cost reduction by developing concentrator solar cells.

Therefore, concentrator 3-junction and 4-junction solar cells have great potential for realizing super high-efficiency of over 40%. As a 3-junction combination, InGaP/InGaAs/Ge cell on a Ge substrate will be widely used because this system has already been developed. The 4-junction combination of an $E_g=2.0\text{eV}$ top cell, a GaAs second-layer cell, a material third-layer cell with an E_g of 1.05eV , and a Ge bottom cell is lattice-matched to Ge substrates and has a theoretical efficiency of about 42% under 1-sun AM0. This system has a potential efficiency of over 47% under 500-suns AM1.5 condition.

We are now challenged to develop low-cost and high output power concentrator MJ solar cell modules for terrestrial applications. Concentrator operation of the MJ cells is essential for their terrestrial applications. Therefore, concentrator MJ and crystalline Si solar cells are expected to contribute to electricity cost reduction for widespread PV applications as well as crystalline Si and thin-film PV as shown in figure 21.

ACKNOWLEDMNTS

This work is partially supported by the Ministry of Education, Culture, Sports, Science and Technology as a part of the Private University Academic Frontier Center Program “Super-High Efficiency Photovoltaic Research Center”, and by the New Energy and Industrial Development Organization, and the Ministry of Economy, Trade and Industry, Japan.

REFERENCES

- [1] Jackson, W.D., *Transactions of the Conference on the Use of Solar Energy 5* Tucson: University of Arizona Press, p.122 (1955).
- [2] Wolf, M., *Proc. IRE* **48**, 1246 (1960).
- [3] Fan, J.C.C., Tsaur, B-Y., and Palm, B.J., *Proceedings of the 16th IEEE Photovoltaic Specialists Conference*, New York: IEEE, p.692 (1982).
- [4] Hutchby, J.A., Markunas, R.J., and Bedair, S.M., “Photovoltaics”, *Proceedings of the SPIE* **543**, p.543 (1985).
- [5] Ando, K., Amano, C., Sugiura, H., Yamaguchi, M., and Salates, A., *Jpn. J. Appl. Phys.* **26**, L266 (1987).
- [6] Sugiura, H., Amano, C., Yamamoto, A., and Yamaguchi, M., *Jpn. J. Appl. Phys.* **27**, 269 (1988).
- [7] Amano, C., Sugiura, H., Yamamoto, A., and Yamaguchi, M., *Appl. Phys. Lett.* **51**, 1998 (1987).
- [8] Olson, J.M., Kurtz, S.R., and Kibbler, K.E., *Appl. Phys. Lett.* **56**, 623 (1990).
- [9] Takamoto, T., Ikeda, E., Kurita, H., Ohmori, M., and Yamaguchi, M., *Jpn. J. Appl. Phys.* **36**, 6215 (1997).
- [10] Yamaguchi, M., Okuda, T., Taylor, S.J., Takamoto, T., Ikeda, E., and Kurita, H., *Appl. Phys. Lett.* **70**, 1566 (1997).
- [11] Brown, M.R., Goldhammer, L.J., Goodelle, G.S., Lortz, C.U., Perron, J.N., Powe, J.S., Schwartz, J.S., Cavicchi, B.T., Gillanders, M.S., and Krut, D.D., *Proceedings of the 26th IEEE Photovoltaic Specialists Conference*, New York: IEEE, p. 805 (1997).
- [12] Takamoto, T., Kaneiwa, M., Imaizumi, M., and Yamaguchi, M., *Progress in Photovoltaics* **13**, 495 (2005).
- [13] King, R.R., Law, D.C., Edmondson, K.M., Fetzer, C.M., Kinsney, G.S., Yoon, T., Sherif, R.A., and Karam, N.H., *Appl. Phys. Lett.* **90**, 183516 (2007).
- [14] Araki, K., Uozumi, H., Egami, T., Hiramatsu, M., Miyazaki, Y., Kemmoku, Y., Akisawa, A., Ekins-Daukes, N.J., Lee, H-S., and Yamaguchi, M., *Progress in Photovoltaics* **13**, 513 (2005).
- [15] Tomita, T., *Proceedings of the 4th World Conference on Photovoltaic Energy Conversion*, New York: IEEE, p.2450 (2006).
- [16] Ahrenkiel, R.K., Keyes, B.M., Durbin, S.M., and Gray, J.L., *Proceedings of the 23rd IEEE Photovoltaic Specialists Conference*, New York: IEEE, p.42 (1993).
- [17] Yang, M.-J., Yamaguchi, M., Takamoto, T., Ikeda, E., Kurita, H., and Ohmori, M., *Solar Energy Materials and Solar Cell* **45**, 331 (1997).
- [18] Yamaguchi, M., and Amano, C., *J. Appl. Phys.* **58**, 3601 (1985).
- [19] Takamoto, T., Agui, T., Kamimura, K., Kaneiwa, M., Imaizumi, M., Matsuda, S., and Yamaguchi, M., *Proceedings of the 3rd World Conference on Photovoltaic Energy Conversion*, Osaka, p 58 (2003).
- [20] Takamoto, T., Yamaguchi, M., Ikeda, E., Agui, T., Kurita, H., and Al-Jassim, M., *J. Appl. Phys.* **85**, 1481 (1999).
- [21] Khan, A., Yamaguchi, M., Bourgoin, J.C., and Takamoto, T., *Appl. Phys. Lett.* **76**, 2559 (2000).
- [22] Lang, D.V., Kimerling, L.C., and Leung, S.Y., *J. Appl. Phys.* **47**, 3587 (1976).